



Cite this: *Chem. Soc. Rev.*, 2022, **51**, 1592

Metal-catalyzed asymmetric heteroarylation of alkenes: diverse activation mechanisms

Shenghan Teng ^{ab} and Jianrong Steve Zhou *^a

This review summarizes the state-of-the-art in transition metal-catalyzed asymmetric alkylation of heteroarenes using alkenes (covering literature from 2000 to late 2021). Based on elementary reactions on metals for substrate activation, these reactions are broadly classified in several categories: (A) concerted oxidative addition of heteroaryl C–H bonds on rhodium(i) and iridium(i), (B) ligand-to-ligand hydrogen transfer (LLHT) on low-valent 3d metal complexes of nickel and cobalt, (C) different ways for deprotonation of heteroaryl C–H bonds by late transition metal complexes, especially palladium, including electrophilic aromatic substitution and a related mechanism, base-assisted intramolecular electrophilic substitution, concerted and nonconcerted metalation deprotonation, (D) σ -bond metathesis by d^0 early transition metal complexes, (E) electrophilic activation of olefins by Pd(II), Pt(II) and Au(I), and (F) metal hydride insertion of aryl olefins and dienes. The demand to achieve enantiocontrol in the heteroarylation reactions has also driven innovation in chiral ancillary ligands, exemplified by extremely bulky, chiral N-heterocyclic carbenes for nickel catalysts, bulky monodentate oxazolines for Wacker-type reactions and chiral cyclopentadienyl ligands for half-sandwich complexes of scandium.

Received 24th August 2021

DOI: 10.1039/d1cs00426c

rsc.li/chem-soc-rev

Key learning points

1. Activation of heteroarenes by concerted oxidative addition of heteroaryl C–H bonds on rhodium and iridium complexes.
2. Ligand-to-ligand hydrogen transfer on 3d late transition metals (nickel, cobalt and iron) that bypasses discrete oxidative addition of C–H bonds.
3. Different mechanisms for deprotonation of heteroarenes to generate heteroaryl metal species under catalytic conditions, such as electrophilic aromatic substitution of indole and pyrrole, concerted and nonconcerted deprotonation–metalations of thiophene, furan and azoles.
4. σ -bond metathesis of pyridine on d^0 half-sandwich complexes of scandium.
5. Wacker-type activation of olefins for attack by nucleophilic heteroarenes and metal hydride insertion of styrene and dienes to produce benzyl and allyl metal complexes.

1. Introduction

Heteroarenes having chiral alkyl chains are key motifs in some medicines and drug candidates (Fig. 1).^{1–4} For example, Galidesivir and Remdesivir are nucleoside analogues which were developed as antiviral agents against hepatitis C and other viral infections. In the recent COVID-19 pandemic, Remdesivir is also used for post-infection treatment of COVID-19 symptoms. Lipitor is a selective inhibitor of HMG–CoA reductase which is being used for the treatment of hypertension by reducing

cholesterol level in blood. Veliparib is used for the treatment of breast cancers and recurrent ovarian cancer, by preventing DNA repair. Epibatidine is an interesting alkaloid extracted from

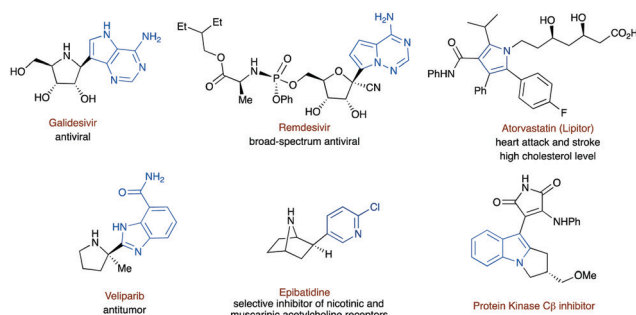


Fig. 1 Examples of chiral alkylated heteroarenes in medicines and natural products.

^a State Key Laboratory of Chemical Oncogenomics, Guangdong Provincial Key Laboratory of Chemical Genomics, School of Chemical Biology and Biotechnology, Peking University Shenzhen Graduate School, Room F312, 2199 Lishui Road, Nanshan District, Shenzhen 518055, China. E-mail: jrzhou@pku.edu.cn

^b Division of Chemistry and Biological Chemistry, School of Physical and Mathematical Sciences, Nanyang Technological University, 21 Nanyang Link, Singapore 637371, Singapore

poison dart frogs, containing an aza[2.2.1]bicycle possessing a chloropyridine substituent. It functions as a potent selective agonist of nicotinic and muscarinic acetylcholine receptors. The research to develop it as an analgesic, however, was eventually abandoned due to unexpected toxicity. One more example is a Protein Kinase C β inhibitor containing a dihydropyrroloindole core.

This review focuses on transition metal-catalyzed asymmetric alkylation of heteroarenes using alkenes, by activating either heteroaryl C–H bonds or olefins. In particular, an emphasis is placed on discussion of reaction mechanisms for activation and mechanistic studies to unravel the activation mechanism. This review does not include enantioselective alkylation of indoles and pyrroles using carbonyl compounds, imines and Michael acceptors which relies on Friedel–Crafts-type reactivity,^{5,6} *via* Lewis acidic metal catalysts and Brønsted acid catalysts. Moreover, the Review does not cover iminium activation of α,β -unsaturated aldehydes and ketones by chiral amines, for addition of indole and pyrrole.

In the last two decades, many catalytic methods have emerged to allow direct incorporation of enantioenriched alkyl fragments onto functionalized heteroarenes.^{7–12} Common alkylating reagents include alkyl halides, alkyl sulfonates and Michael acceptors, as well as unactivated olefins. Olefins are readily accessible and remain unreactive under many other reaction conditions. Under suitable reaction conditions, olefins are activated for insertion or external nucleophilic attack. They are also atom-economic alkylating agents without producing by-products themselves in principle.

Unsaturated heteroarenes are easily accessible or readily prepared, but their innate reactivity and regioselectivity issues need to be addressed during alkylation. In comparison, (hetero) aryl halides and sulfonates are often used in crosscouplings with alkylating reagents (*e.g.*, alkyl-9-BBN), but these electrophiles are prepared indirectly from (hetero)arenes or (hetero)aryl alcohols. Alternatively, alkyl couplings of (hetero)aryl

organometallic reagents or boron reagents can be used, but these reagents need to be prepared beforehand and the preparative procedures may be incompatible with sensitive structures or polar functional groups.

In the studies of metal-catalyzed reaction mechanisms, DFT calculations are now often employed in combination with experimental investigation to examine different reaction pathways. Deuterium labelling and kinetic isotope effect (KIE) have proven to be indispensable tools in this regard.¹³ The distribution of deuterium in starting materials and products often provide insights into reversibility of individual steps in catalytic cycles, while KIE values reveal whether a particular step of interest, which is usually involved in bond activation or bond formation, contributes to the overall rate of a catalytic reaction. Moreover, DFT calculations are now routinely performed on whole systems including entire chiral catalysts, owing to dramatic increase in computational power over the last two decades.^{14,15} The calculations allow direct first-hand glimpse into different putative pathways. They give hints in first approximation if all the steps in a tentative catalytic cycle are energetically feasible and if a certain step is rate-limiting (judged from heights of activation barriers) or stereo-determining in the entire catalytic cycle.

Several organometallic reaction mechanisms were well-established prior to 2000, for example, electrophilic palladation, σ -bond metathesis of (hetero)aryl C–H bonds on electron-deficient d^0 early metal ions and lanthanides and Wacker-type activation of alkenes by Group-10 metal ions. More importantly in the last two decades, several new elementary mechanisms have been discovered through experiments and calculations which have been utilized in selective activation of C–H bonds in (hetero)arenes. Such examples include regioselective oxidative addition of heteroaryl C–H bonds on low-valent rhodium and iridium complexes; ligand-to-ligand hydrogen transfer on 3d metals such as nickel and cobalt; both concerted and nonconcerted metalation deprotonations of (hetero)aryl C–H bonds,



Shenghan Teng

Dr Shenghan Teng was born in Fuzhou, China. He received his BS and MS degrees in Chemistry from the East China Normal University under the guidance of Prof. Wenhao Hu. In 2016, he conducted his PhD studies in Prof. Jianrong Steve Zhou's group at Nanyang Technological University. He is currently a research fellow with Prof. Teck-Peng Loh at NTU where he works on green organic reactions in water. He is the recipient of 2021 SNIC-Prof Lee Soo Ying Young Chemist Gold Award.



Jianrong Steve Zhou

Prof. Jianrong Steve Zhou was born in Ningbo, China. He received BSc and Master's degrees at the National University of Singapore under the tutelage of Prof. Teck-Peng Loh (1994–2000). He then pursued doctoral studies in the lab of Prof. Gregory Fu at MIT (2001–5) and received postdoctoral training in organometallic catalysis in Prof. John Hartwig's lab at Yale University and UIUC (2005–8). In 2008, he started independent research career at Nanyang Technological University as Assistant Professor. In 2019, he relocated to Peking University Shenzhen Graduate School. His research interests include transition metal-catalyzed stereoselective reactions such as asymmetric Heck-type reactions and transfer hydrogenation.

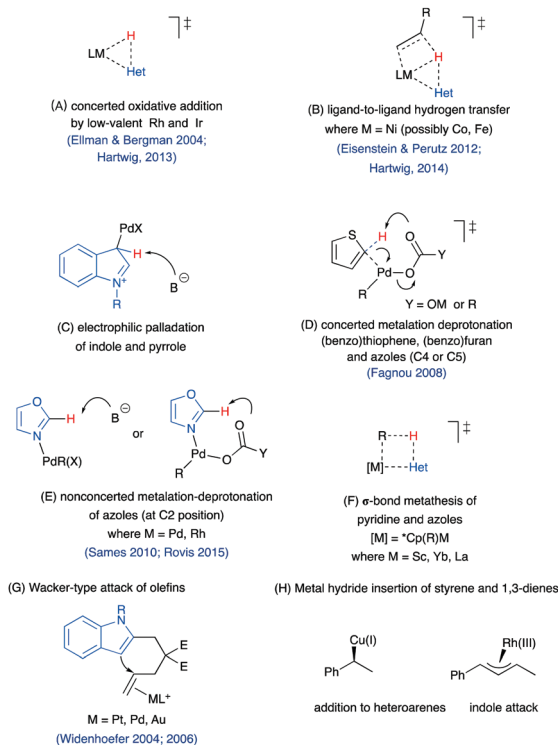


Fig. 2 Overview of activation modes in asymmetric alkylation of heteroarenes using alkenes: key transition states responsible for C–H bond activation (A–F); a key intermediate in electrophilic activation of alkenes (G); benzyl and allyl complexes produced from metal hydride insertion of styrene and 1,3-dienes (H).

mostly on palladium(II) complexes and other late metal complexes. These discoveries represented some of the forefronts in organometallic chemistry and catalysis in the last two decades.

It should be pointed out that over the last decade, C–H bond activation by transition metal complexes have been subjected to extensive investigations by DFT calculations, which have revealed several new pathways and also shed light on their subtle dependence on transition metals, oxidation states, ancillary ligands and nature of bases.^{16–19}

Collectively, a “toolbox” of mechanistic tools is available today for selective activation of heteroarenes and alkenes to allow enantioselective carbon–carbon bond formation (see Fig. 2 with the names of discoverers and years of recent discoveries shown):

(A) In the activation of C–H bonds of heterocycles by low-valent complexes of rhodium(I), Rh–H insertion of olefins is followed by C–C reductive elimination to release products. Iridium(I) catalysts, however, operate *via* an alternative sequence involving Ir–C insertion of alkenes and C–H reductive elimination to release final products. The reason for the difference is believed to be prohibitively high barriers of C–C reductive elimination on iridium(III) centers.

(B) As an exciting discovery, a new pathway of LLHT has gained wide acceptance today in nickel(0)-catalyzed alkylation of arenes and heteroarenes using alkenes. Compared with 4d and 5d heavier congeners, 3d late transition metals generally form shorter and weaker bonds with ligands, which help to

bring substrates closer for the one-step transfer of a hydrogen atom from the (hetero)arene to alkene. The alternative pathway of concerted oxidative addition of C–H bonds is prohibited owing to the instability of oxidative-addition complexes of nickel. Low-valent cobalt and iron complexes can adopt this pathway, too.

In deprotonation of heterocycles by late metal ion complexes, different mechanisms may operate: (C) electrophilic aromatic substitution generally operates on indoles and pyrroles with high intrinsic nucleophilicity. (D) Concerted metalation–deprotonation is common for many types of heteroarenes by palladium (and rhodium) carboxylates, carbonates and phosphates. (E) Nonconcerted metalation–deprotonation has recently gained acceptance in chemical community for the activation of azoles at C2 positions (next to nitrogen atoms).

(F) The d^0 early transition metal complexes, *e.g.*, scandium and lanthanides, can activate C2–H bonds in pyridines *via* σ -bond metathesis.

(G) In activation of olefins by electrophilic metal complexes of Pt(II), Pd(II) and Au(I), nucleophilic heteroarenes (typically, indole) undergo Wacker-type *anti*-attack of bound alkenes. Today, enantioselective cyclization of indoles with tethered olefins has been achieved by chiral Pt(II) and Au(I) complexes. One example of recent advancement in this area is the development of chiral monodentate oxazoline ligands which have successfully enabled intermolecular, enantiofacial attack of indole on olefins (tethered to an *N*-quinolyamide). Notably, a palladium catalyst ligated by a weakly donating MeO–biphep also allowed asymmetric Wacker-type three-component coupling of cycloalkenes, heteroarenes and propargylic acetates.

(H) Chiral metal hydride complexes can insert selectively on one π -face of styrene and conjugated dienes, which can serve as an entry point of olefins in catalysis. The resulting enantiotopic benzyl or allyl complexes may be intercepted by either nucleophilic indoles or electrophilic azine derivatives. We believe more examples of this kind will emerge in future.

2. Oxidative addition of heteroaryl C–H bonds to low-valent late metals and related ligand-to-ligand hydrogen transfer

One common way to activate heteroarenes is concerted oxidative addition of heteroaryl C–H bonds by low-valent late transition metals such as rhodium and iridium. The resulting heteroaryl metal hydride then underwent insertion of hydride or heteroaryl ligand to olefins followed by C–C or C–H reductive elimination to form the alkyl–heteroaryl bond. In recent years, a variant of the reaction mechanism was discovered that allowed concomitant oxidative addition and hydride insertion to alkenes (ligand-to-ligand hydrogen transfer), without forming discrete heteroaryl metal hydride species.

2.1 Oxidative addition of heteroaryl C–H bonds

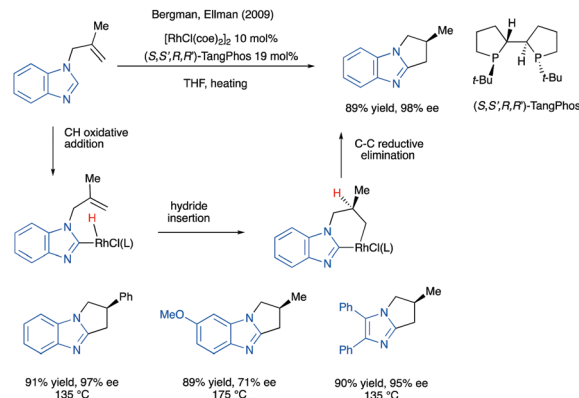
Back in 1997, Murai *et al.* reported the first example of rhodium-catalyzed asymmetric cyclization of pendent olefins

Tutorial Review

via directed activation of alkenyl C–H bonds; the ees were as high as 87% in the presence of imidazole directing groups.²⁰ Low-valent rhodium complexes are known to readily undergo oxidative addition of aryl and heteroaryl C–H bonds, especially when *ortho*-directing groups are present.^{21,22} For example, rhodium(i) complexes promoted imine-directed oxidative addition of *ortho* C–H bonds of arenes and indoles; subsequent hydride insertion and final C–C reductive elimination afforded benzofused products (Scheme 1A).²³ The last step of C–C reductive elimination was rate-limiting, hence the need of high reaction temperatures in some cases. The method was later applied to a concise synthesis of a Protein Kinase C β inhibitor (Scheme 1B).²⁴

In the cyclization of benzimidazoles, no directing group was needed, owing to temporary binding of azacycles to Rh(i) (Scheme 2).²⁵ Since benzimidazoles can compete well with weakly donating phosphorus ligands for binding to late metal centers, a strongly donating di(alkylphosphine), TangPhos, was used to replace weakly coordinating phosphoramidites.

Iridium(i) complexes were known to undergo oxidative addition of C–H bonds of arenes and heteroarenes.²⁶ In C2-selective alkylation of indole using activated norbornene, no directing group was needed.²⁷ It was interpreted that facile reversible oxidative addition of indolyl N–H bonds helped to recruit the iridium(i) catalyst, which at a higher temperature also underwent reversible oxidative addition of neighboring indolyl C–H bonds, which was trapped by rate-limiting olefin insertion (Scheme 3). This reactivity was broadly applicable to heterocycles such as furans, thiophenes, pyrroles and benzofused derivatives. Oxidative addition of the indolyl C2–H bond on iridium(i) was found to proceed at room temperature, but Ir–C insertion of norbornene didn't occur until the temperature was raised to 100 °C. When reactive norbornene was changed to 1-octene, Markovnikov-type

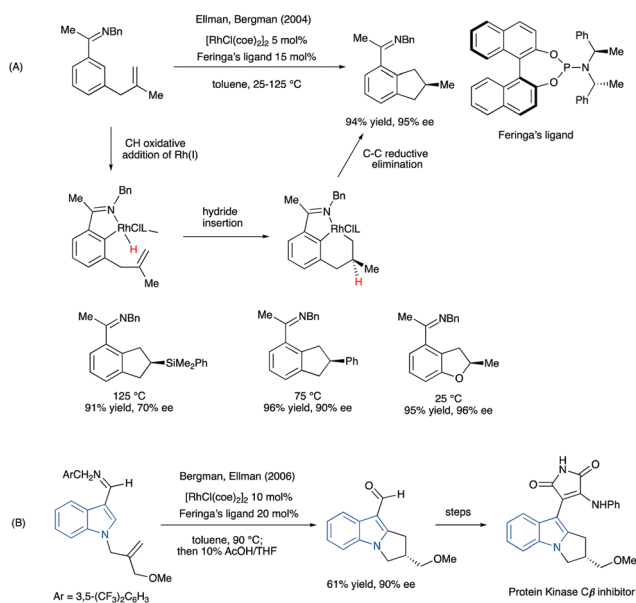


Scheme 2 Rh(i)-catalyzed *endo*-selective cyclization of benzimidazoles.

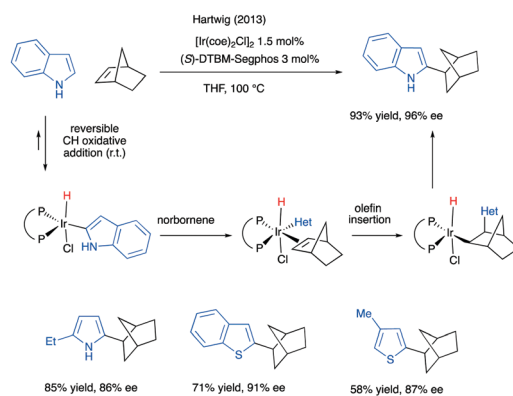
hydroamination occurred instead, because the Ir–N insertion is faster than the Ir–C insertion.²⁸

Hydroxoiridium(i) complexes of dienes can catalyze selective *ortho*-alkylation of *N*-sulfonyl benzamides using alkyl vinyl ethers. The reactivity can be extended to 2-thienyl and 2-furanyl amides (Scheme 4A).²⁹ A deuterium-labelling experiment of a benzamide derivative in the presence of deuterated water revealed that extensive deuteration occurred on the *ortho* sites of benzamide and vinyl ether (Scheme 4B). The hydroxoiridium(iii) species was probably converted to a deuteride complex *via* σ -bond metathesis with deuterated water. Thus, *ortho* C–H oxidative addition was believed to be reversible; so was Ir–H insertion to olefins, but the insertion was nonproductive as an off-cycle equilibrium owing to difficult C–C reductive elimination from Ir(iii). Overall, the productive pathway involved a sequence of rate-limiting aryl insertion of olefins and C–H reductive elimination.

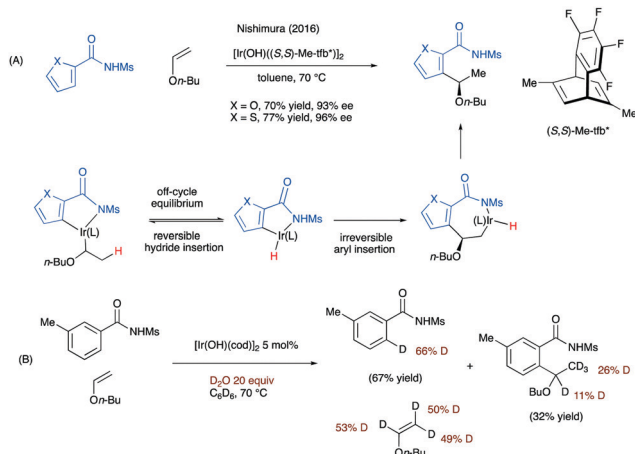
A similar *ortho*-alkylation of 3-*N*-amidothiophenes was reported with styrene and α -olefins (Scheme 5).³⁰ The innovation of two weakly donating chelators, a ferrocene-derived diphosphinite and a Kelliphite-type diphosphite, which can form deep chiral packet upon metal chelation, enabled highly stereoselective insertion of terminal olefins, a true feast in chiral ligand design! The latter was used in the reactions of *N*-acylanilines and an *N*-acetamidoindole.



Scheme 1 Rh(i)-catalyzed imine-directed cyclization of arenes and indoles with tethered alkenes.

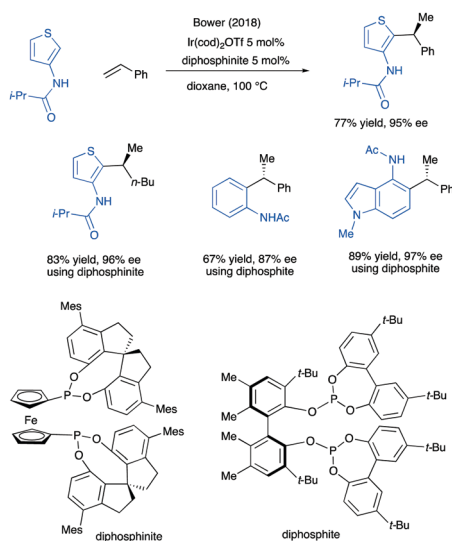


Scheme 3 Ir(i)-catalyzed enantioselective hydroheteroarylation of norbornene.



Scheme 4 Asymmetric alkylation of *N*-sulfonylbenzamides with alkyl vinyl ethers enabled by a (diene)iridium complex.

A comparison of Rh- and Ir-catalyzed examples above suggests that aryl–alkyl reductive elimination is energetically feasible from Rh(III), but not from Ir(III). A similar trend of C–C reductive elimination was implied in Rh- and Ir-catalyzed hydroalkylation of enamides using alkenes, as discovered by Dong *et al.*,^{31–33} and hydroalkynylation of enamides reported by Li *et al.*^{34,35} According to DFT calculations,^{36–38} the Rh–C bond is generally weaker than the iridium counterpart owing to relativistic effect of iridium. Rh prefers to be in Rh(I), while Ir prefers oxidation state of +3. The instability of C–H oxidative adducts of Rh(III) leads to unfavorable high-energy transition states for Rh–C insertion of alkenes. Owing to the reversibility of Ir–H insertion of alkenes, the Ir-catalyzed processes can avoid energetically prohibitive C–C reductive elimination and proceed through Ir–C insertion and Ir–H reductive elimination to form final products.



Scheme 5 Enantioselective alkylation of *N*-acylanilines and *N*-acylthiophene with styrenes and α -olefins.

2.2 Ligand-to-ligand hydrogen transfer

Back in 2012, in studies of nickel-catalyzed hydroarylation of alkynes with fluoroarenes, Eisenstein and Perutz first suggested LLHT was more consistent with observed KIE values of close to unity than classical oxidative addition followed by alkyne insertion.³⁹ Today, the so-called “ligand-to-ligand hydrogen transfer” (LLHT) has gained strong foothold in nickel- and cobalt-catalyzed hydro(hetero)arylation of both alkynes and alkenes, based on a body of mechanistic evidence and DFT calculations. The LLHT occurs directly between metal-bound (hetero)arenes and alkynes/alkenes *via* a single transition state, rather than two discrete steps of classical concerted oxidative addition and insertion of unsaturated bonds. The gist is that the LLHT bypasses high-energy oxidative adducts of nickel and cobalt in these catalytic cycles.

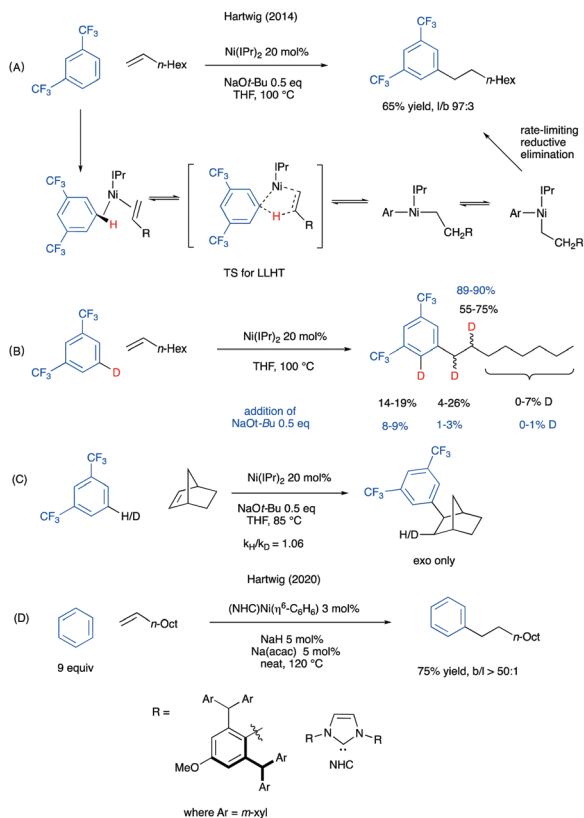
In nickel(0)-catalyzed hydroarylation of terminal alkenes that preferentially add linear alkyl groups to activated arenes, an intrinsic KIE value was found to be close-to-unity, which was considered to be consistent with the LLHT if the step of hydrogen transfer between aryl C–H bonds and alkenes is reversible (Scheme 6A).⁴⁰ (NHC)Ni(0) complexes also catalyzed intermolecular hydroheteroarylation of alkenes using indoles, pyrroles and (benzo)furans, in which the C–H bonds next to the heteroatoms were selectively activated.⁴¹ The preference for LLHT on (NHC)Ni(0) complexes over concerted oxidative addition stems from the smaller atomic radius of Ni and smaller Ni(II)–H bond energy than those of Pd and Pt analogues. Moreover, the bulky NHC ligand on nickel(0) complexes also accelerates LLHT by decreasing the distance between the bound arenes and alkenes.⁴²

In deuterium-labeling experiments, an appreciable deuteration was detected at both C1 and C2 positions of the product, which was caused by a reversible LLHT processes (Scheme 6B). Consistent with this scenario, sodium *t*-butoxide, which can remove presumably off-cycle nickel hydride species, significantly suppressed the extent of deuterium scrambling in products. Furthermore, the hydroarylation with norbornene involved almost quantitative transfer of the deuterium to its *exo*-position, with a competitive KIE effect of 1.06 (Scheme 6C). Moreover, DFT calculations revealed high instability of the putative oxidative-addition complex of (NHC)Ni(Ar)(H). Therefore, it was concluded that the primary-over-secondary alkyl selectivity in products originated from the selectivity in aryl–alkyl reductive elimination from nickel(II) which is irreversible.

Further engineering of extremely bulky NHC ligands on the nickel catalysts enabled common unactivated arenes such as benzene to couple and also raised the regioselectivity to favor almost exclusively primary-alkyl coupling products (Scheme 6D).⁴³ Interestingly, DFT calculations shed light on the beneficial roles of noncovalent attractive interactions. The interactions of peripheral xyl groups of NHC with the nickel center lowered the barrier of C–C reductive elimination, *via* attractive electrostatic interactions of peripheral xyl rings, London dispersive effect and diminished distortional energy with multiple methyl groups of the xyl rings.

These mechanistic insights above laid the foundation for subsequent invention of chiral NHCs for the purpose of achieving asymmetric hydro(hetero)arylation. For example, a

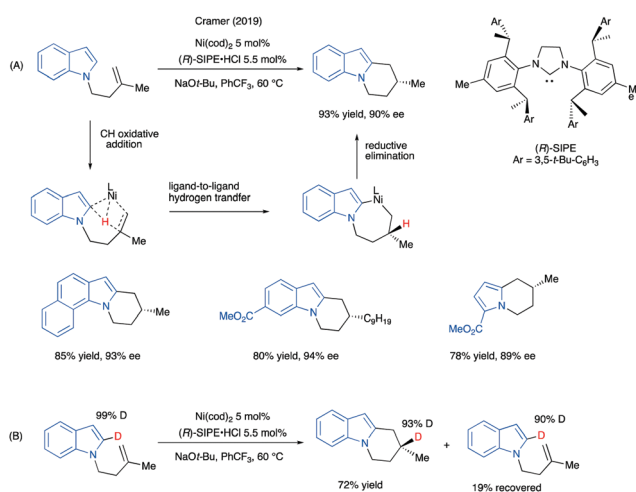
Tutorial Review



Scheme 6 Ni(0)-catalyzed linear-selective hydroarylation of terminal alkenes via LLHT.

bulky, C_2 -symmetric NHC carrying four homochiral 2-phenylethyl groups successfully enabled 6-*endo*-cyclization of indoles and pyrroles in excellent ees (Scheme 7).⁴⁴ Almost quantitative deuterium transfer from the indole ring to the alkene fragment was observed.

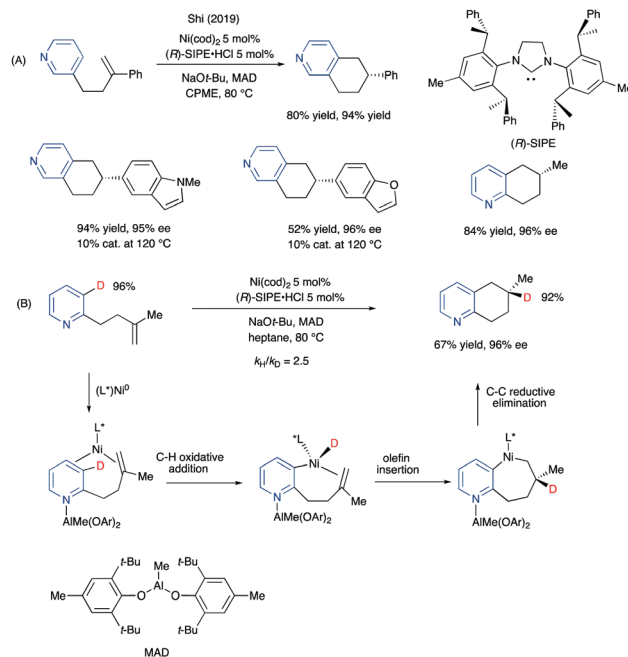
In 2019, Shi *et al.* reported a nickel(0)-catalyzed 6-*endo*-selective alkylation of pyridines. A bulky Lewis acid MAD was used to bind



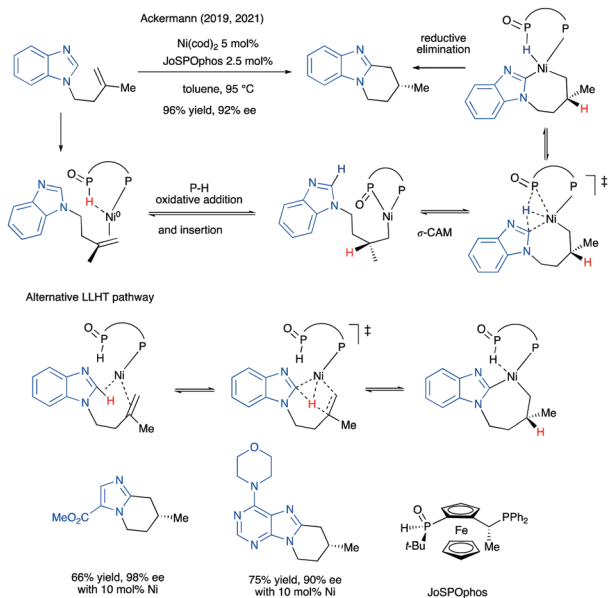
Scheme 7 Enantioselective cyclizations of indoles and pyrroles with tethered olefins enabled by (NHC)Ni catalysis.

to pyridine and shield its C2 positions from reacting (Scheme 8A).⁴⁵ The large N-heterocyclic carbene SIPE helped to forge an effective chiral environment. It also enabled an analogous enantioselective hydroarylation of polyfluoroarenes.⁴⁶ Apparently, the site of C–H cleavage was dictated by temporary binding of nickel to the pendent olefin group. Notably, almost quantitative transfer of the deuterium was observed from pyridine to the product (Scheme 8B). Moreover, a KIE value of 2.5 was observed in a competition experiment using both protio- and deuteriopyridines in one vessel, revealing that the C–H cleavage contributed to the overall rate. Shi *et al.* deemed that the result contradicted with a reversible LLHT and thus, a two-step sequence was proposed (see Scheme 8B). But it is possible under some conditions, the LLHT does not necessarily have to be reversible and therefore, gives a KIE value greater than one. For example, in 2016 Nakao *et al.* reported a KIE value of 3.7 in a Ni-catalyzed *para*-selective alkylation of benzamide with alkenes.⁴⁷

In 2019, Ackermann *et al.* reported that a nickel catalyst ligated by JoSPOphos promoted 6-*endo*-trig cyclization of (benz) imidazoles with pendent alkenes (Scheme 9).⁴⁸ In 2021, Ackermann *et al.* revised the reaction mechanisms by taking into additional information from DFT calculations.⁴⁹ The LLHT was an energetically viable pathway in the nickel catalysis, rather than previously proposed oxidative addition of azacyclic C–H bonds owing to the instability of oxidative adducts, nickel hydride complexes. Another pathway was also energetically feasible based on calculations—a sequence of P–H oxidative addition and hydride insertion is followed by σ -complex-assisted metathesis (σ -CAM)⁵⁰ to activate the benzimidazolyl C–H bond; this sets the stage for a rate-limiting and stereo-determining C–C reductive elimination to release the products.



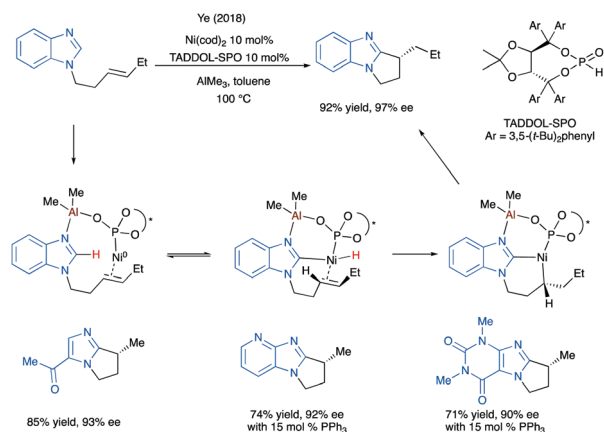
Scheme 8 Enantioselective *endo*-selective cyclization of pyridines with tethered alkenes catalyzed by a (NHC)Ni complex.



Scheme 9 *endo*-Selective cyclization of alkene-tethered benzimidazoles enabled by nickel-JoSPOphos catalyst.

The latter pathway is more consistent with the experimentally observed enantioselectivity. In the σ -CAM, the secondary phosphide of JoSPOphos acted as an internal base to deprotonate benzimidazoles *via* a four-membered transition state to produce nickel azolyl species. The σ -CAM process is assisted by the relatively large size, significant nucleophilicity and polarizability of the phosphide on the metal complex.

In another example of nickel-catalyzed heteroarylation of pendent olefins, a secondary phosphine oxide derived from TADDOL was used as chiral inducer. A KIE of value close to unity was recorded. Ye *et al.* proposed that the benzimidazole C–H bonds were activated by either classical oxidative addition or LLHT (Scheme 10).⁵¹ Based on the observed *exo*-trig cyclization, the authors of this Review suggest that the pathway of oxidative addition is more likely, which allows hydride addition to the distal



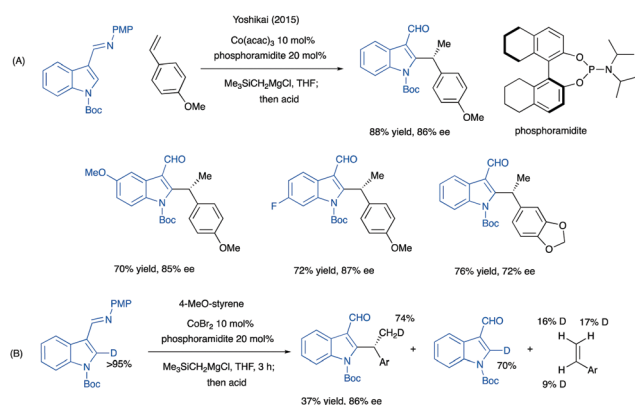
Scheme 10 Asymmetric nickel-catalyzed *exo*-selective cyclization of alkene-tethered benzimidazoles.

site of the tethered alkene, without invoking a high-energy transition state.

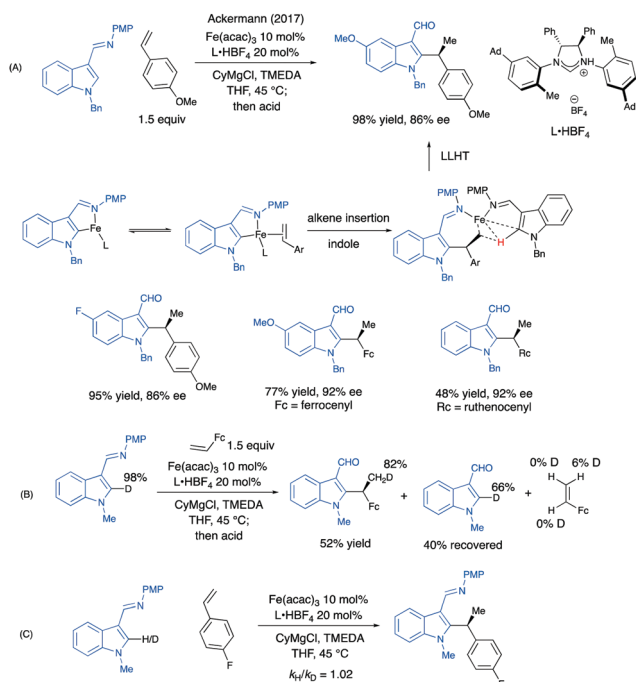
In 2015, Petit *et al.* reported that $\text{Co}(\text{PMe}_3)_4$ promoted *ortho*-alkenylation of arenes using internal alkynes in the presence of imine directing groups *via* a LLHT mechanism.⁵² Recently, Yoshikai *et al.* also reported that low-valent cobalt complexes catalyzed regioselective alkenylation of azacycles using internal alkynes, when the azacycles (*e.g.*, pyridines, pyrimidines, imidazo[1,2-*a*]pyridines, azoles, *etc.*) were activated by metal Lewis acids such as AlMe_3 , $\text{Ti}(\text{O}i\text{Pr})_4$ and ZnPh_2 .⁵³ The reaction most likely proceeded *via* LLHT, therefore drawing an interesting parallelism with the above-mentioned alkenylation reactions of arenes catalyzed by another 3d metal, cobalt.

In 2015, Yoshikai *et al.* also disclosed that low-valent cobalt catalysts, generated *in situ* from reduction of cobalt salts by alkyl Grignard reagents, catalyzed imine-directed enantioselective addition of indoles to styrenes (Scheme 11A).⁵⁴ In deuterium labelling experiments, an appreciable amount of deuterium was washed out from the indole, while extensive deuterium was washed into the recovered alkene (Scheme 11B). Thus, a pathway was proposed, consisting of two reversible steps of *ortho* C–H oxidative addition and olefin insertion, followed by irreversible C–C bond formation. In retrospect, an LLHT pathway is more likely.

In an iron-catalyzed process reported by Ackermann *et al.*, a KIE value of close to unity was used to suggest a reversible LLHT pathway to release the products from an alkyl iron(i) species after styrene insertion (Scheme 12).⁵⁵ In the experiment, C2-deuterated indole gradually lost its isotope over time (66% deuterium in the recovered material), but only 6% deuterium was scrambled into the recovered alkene. The fate of the lost deuterium remains unclarified. The authors proposed, based on experiments and DFT calculation, that the reaction proceeded *via* reversible metalation of the indole and irreversible olefin insertion. It should be noted that the LLHT between alkyl iron species and another molecule of indole released the final product, during which the oxidation state of iron(i) remained unchanged.



Scheme 11 Co-catalyzed imine-directed alkylation of indoles with styrenes.



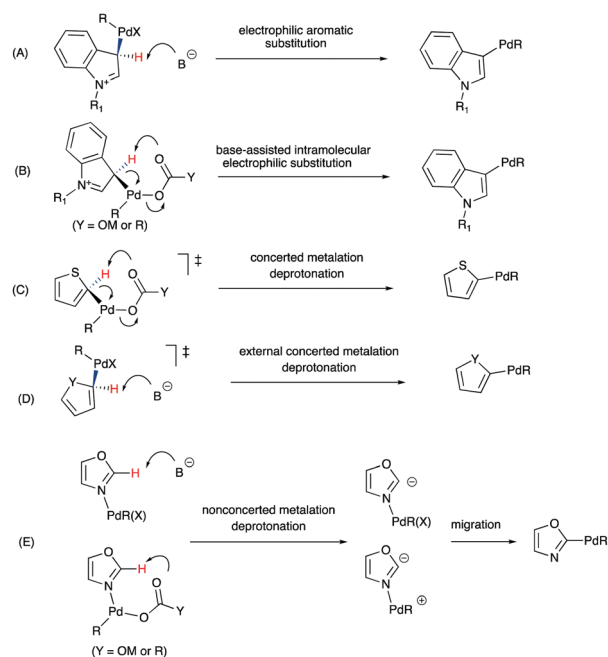
Scheme 12 Fe-catalyzed imine-directed alkylation of indoles.

3. Deprotonation of heteroarenes *via* electrophilic aromatic substitution, concerted metalation–deprotonation (CMD) and nonconcerted metalation–deprotonation (*n*CMD)

Several reaction mechanisms have been delineated for the deprotonative metalation of unsaturated (hetero)arenes by transition metal ions (Scheme 13).⁴⁹ In conjunction with experiments, DFT calculations have contributed significantly to our understanding of different modes of C–H activation and their ramifications in catalytic processes as follows.

(a) Electrophilic aromatic substitution or specially in palladium-mediated reactions, electrophilic palladation (Scheme 13A). The pre-equilibrium between electrophilic metal centers and electron-rich (hetero)arenes, such as indole and pyrrole, forms Wheland-type complexes which contain highly acidic *ipso*-C–H bonds. The latter then lose a proton to form (hetero)aryl–metal bonds. In the case where electron-rich arenes prove to be preferred substrates and the bases become bound to the metal centers (*e.g.*, carboxylates), this mechanism is now called “base-assisted intramolecular electrophilic substitution” (BIES). It is operating, more frequently than previously recognized, in many catalytic C–H activation processes in which carboxylates, phosphates and carbonate anions are used (Scheme 13B).^{56–58} This mechanism was termed by Carrow *et al.* as electrophilic CMD (eCMD).^{59,60}

(b) In 2008, Fagnou and Gorelsky coined the term “concerted metalation deprotonation” (CMD), which refers to the metalation of C–H bonds in which a metal–carbon bond forms at the same time that the C–H bond is deprotonated by a base through a



Scheme 13 Several reaction mechanisms for the deprotonation of heteroarenes by Pd(II) complexes.

single transition state.^{61,62} In most examples, the base is a carboxylate, phosphate or carbonate ligand bound to the metal center and the deprotonation proceeds via a six-membered transition state (Scheme 13C). Around the same time, Davies and Macgregor coined another nomenclature “ambiphilic metal ligand activation” (AMLA), which emphasizes on synergistic effect of electrophilic metal centers and internal bases (*e.g.*, carboxylate ligands) during deprotonation of C–H bonds.^{63,64} So CMD with an internal base is also denoted as AMLA/CMD. In 2017, Davies and Macgregor provided a detailed review on DFT studies of carboxylate-assisted C–H activation by Groups 8–10 metal complexes.⁶⁵ In other cases in which the base is fully dissociated from the metal centers (an external base), *e.g.*, a trialkylamine or tetramethylguanidine, the term “external CMD” is designated (Scheme 13D).

The CMD or AMLA/CMD has been reported for alkylation at C2 position of heteroarenes, *e.g.*, pyridine *N*-oxide, thiophene, furan and benzofused ones, by anionic ligands, typically by Pd(II)-bound carboxylates, carbonates and phosphates.^{59,62,66} This mechanism was also reported for deprotonation of azoles at C4 or C5 positions and pyridines.

(c) A new mechanism of nonconcerted metalation–deprotonation (*n*CMD) is recently established for palladation at C2 positions of azoles (Scheme 13E).^{67,68} The nitrogen coordination activates neighboring C–H bonds for the deprotonation by external bases or by a bound carboxylate, carbonate or phosphate. The deprotonation produces a carbene-type species, which is quickly followed by N→C migration to produce metal azolyl species.

The two mechanisms, electrophilic aromatic substitution, concerted metalation–deprotonation, differ from each other in the timing of the carbon–metal bond formation and loss of

proton. The *n*CMD is supported by good coordinating ability of azolyl nitrogen to transition metals and reasonable stability of the intervening carbene-like species.

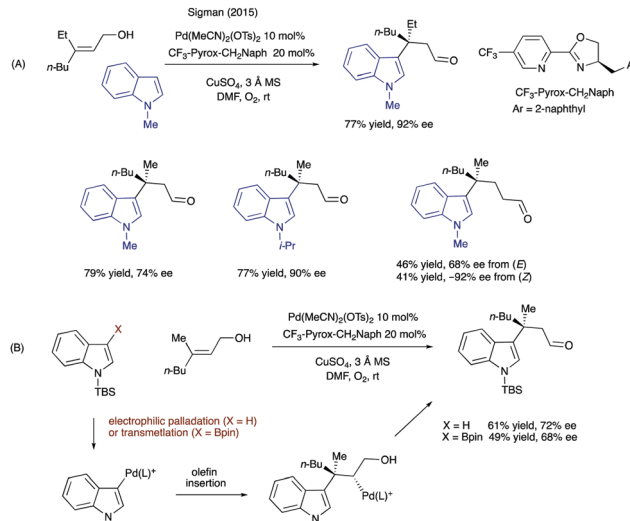
3.1 Electrophilic aromatic substitution of indoles and pyrroles or base-assisted intramolecular electrophilic substitution

Electrophilic Pd(II) complexes can readily react with electron-rich heteroarenes such as indoles and pyrroles to form heteroaryl palladium species followed by deprotonation by an external base. The deprotonation is often found to be reversible. Subsequent *syn*-insertion of alkenes then allows construction of tertiary and quaternary stereocenters. Today, Fujiwara-Moritani-type reaction is one of the earliest examples of the so-called cross-dehydrogenative couplings (CDC).

In 2003, palladium-catalyzed annulations were reported between indoles and pendent olefins in the presence of a weak donor, ethyl nicotinate (Scheme 14A).⁶⁹ In the addition of indole to a disubstituted cyclohexene, the C–C bond formation occurred *syn* to an eliminable allylic hydrogen. The *syn*-carbopalladation led to the formation of a single diastereomer, whose configuration was established by NOE analysis.

Later, Sasai *et al.* achieved an enantioselective variant using a weakly donating bis(isooxazoline) (Scheme 14B).⁷⁰ Thus in both cases, weak donation by the nitrogen ligands proved crucial to electrophilic activation of trisubstituted alkenes. It should be pointed out that in both examples in Scheme 14, the presence of acetate and trifluoroacetate ions likely switches the reaction pathway from classical electrophilic palladation to the BIES.

In 2015, Sigman *et al.* disclosed intermolecular asymmetric indole addition to alkenes, by extending catalytic Heck manifolds developed by the same group using palladium catalysts of weakly donating Pyrox ligands (Scheme 15A).⁷¹ The oxidative Heck indoloylation of trisubstituted (homo)allylic alcohols produced



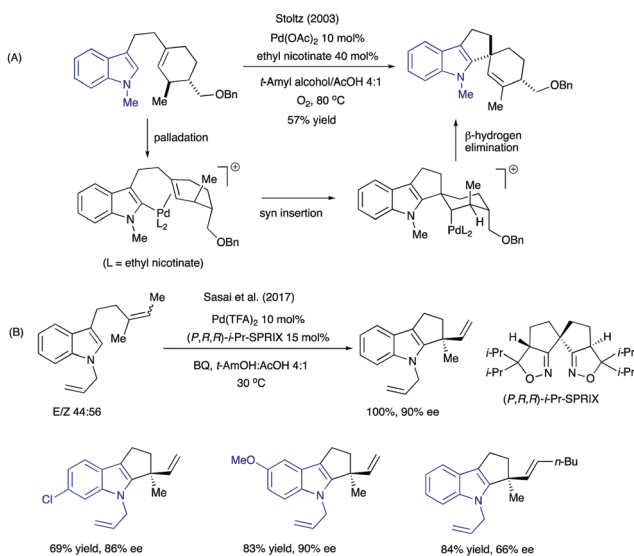
Scheme 15 Pd(II)-catalyzed enantioselective indole addition to trisubstituted (homo)allylic alcohols.

chiral aldehydes bearing quaternary stereocenters. Notably, a (*Z*)-isomer of an alkenol gave higher stereoselectivity than the corresponding (*E*)-isomer (–92% ee vs. 68% ee). The dependence on olefinic geometry is consistent with previous observations in asymmetric oxidative Heck reaction of arylboronic acids previously reported by the Sigman group.⁷² When 3-Bpin-indole was used in place of the parent *N*-silylindole, it gave the adduct in similar enantiomeric excess, thus suggesting that an identical indolyl palladium species was generated *via* electrophilic palladation (Scheme 15B). Following *syn*-insertion, chain walking *via* iterative β -hydride insertion and β -elimination provided aldehydes as final products. Both examples of Scheme 15 probably proceeded *via* electrophilic palladation of indoles as previously proposed, in the absence of carboxylates.

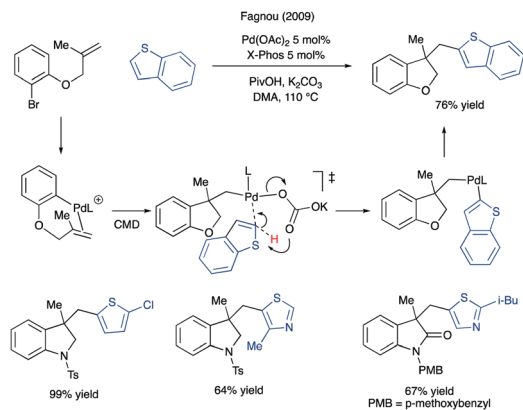
3.2 Concerted metalation–deprotonation (CMD) and nonconcerted metalation–deprotonation (*n*CMD)

Common arenes and heteroarenes such as thiophenes and furans can be readily deprotonated by a palladium(II) complexes of carboxylates, carbonates and phosphates, *via* concerted metalation–deprotonation (CMD). The coordination to the electrophilic Pd(II) centers acidifies the aryl C–H bonds by a few units in the 6-membered transition state. Some azoles can also be activated at C4 or C5 positions *via* CMD at high temperature. Thus, alkyl palladium species, generated from intramolecular Heck-type carbopalladation of olefins, can activate heteroarenes *via* CMD in the construction of alkyl–heteroaryl bonds. In examples reported by Fagnou,^{73,74} thiophene, benzothiophene and thiazole were readily deprotonated by organopalladium carbonates, which are weak bases, for C–C coupling with these heteroarenes (Scheme 16).

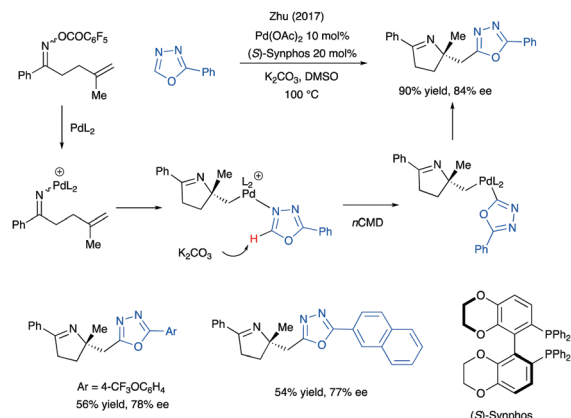
Azoles such as oxazoles and oxadiazoles carry weakly acidified C–H bonds next to heteroatoms and its detailed mechanism of deprotonation by Pd(II) catalysts is distinct from CMD. Coordination of azoles *via* basic nitrogen atoms activates them towards deprotonation by palladium(II) carboxylates, carbonates



Scheme 14 Asymmetric oxidative addition of indoles to alkenes *via* Pd(II) catalysis.

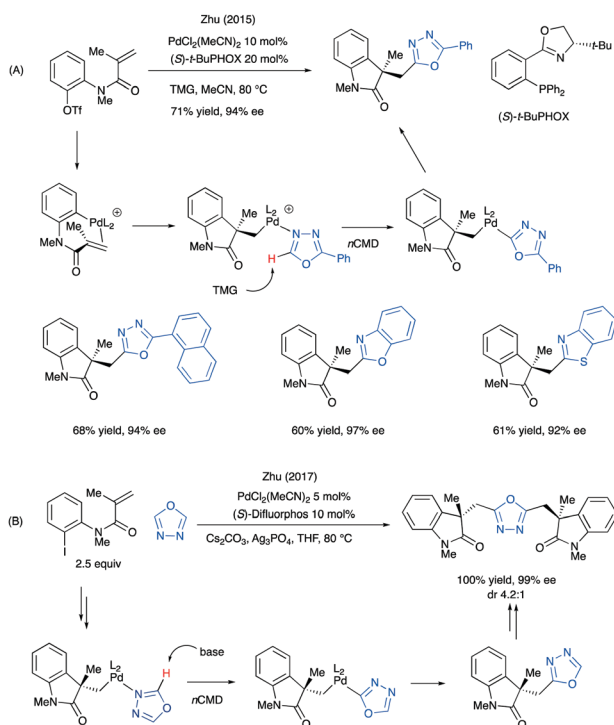


Scheme 16 Domino Heck arylation and coupling with azoles.



Scheme 18 Asymmetric domino Narasaka–Heck iminylation and C–C coupling of oxadiazoles.

or external bases (*n*CMD).⁷⁵ In 2015, Zhu *et al.* reported enantioselective domino carbopalladation and azole coupling to prepare C3-disubstituted oxindoles (Scheme 17A).⁷⁶ After Heck cyclization, azoles were activated by coordination to organopalladium complexes and then deprotonated by a relatively strong organic base tetramethylguanidine (TMG). The weakly donating property of phosphino-oxazoline (PHOX) also helped in activation of azoles (*e.g.*, oxadiazoles, benzoxazoles and benzothiazoles). The reaction was applied to the synthesis of (+)-Esermethole. As an extension of this work, asymmetric double alkylation of 1,3,4-oxadiazole was also achieved under the modified conditions which enabled enrichment of homochiral adducts in the expense of diastereomers (Scheme 17B).⁷⁷



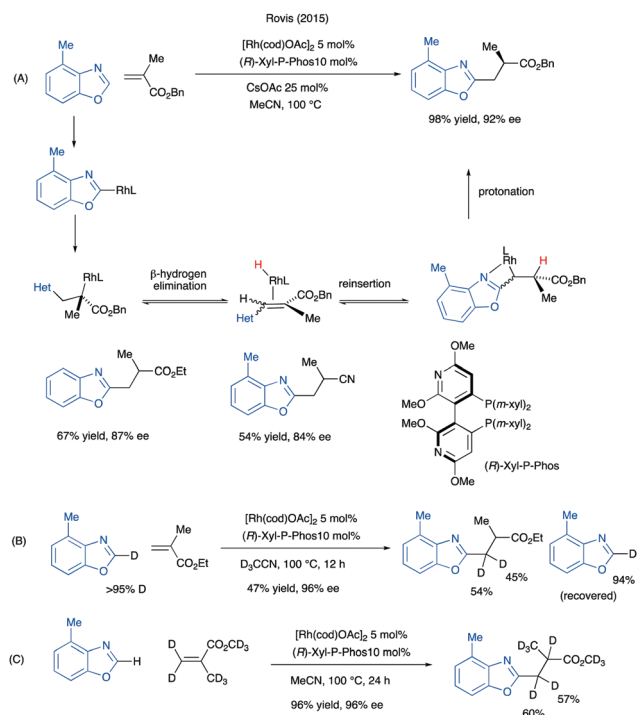
Scheme 17 Asymmetric domino Heck arylation and C–C coupling with azoles.

The same group also reported that a Pd/Synphos catalyst promoted asymmetric domino iminopalladation and couplings with oxadiazoles (Scheme 18).⁷⁸ 2-Substituted oxadiazoles have relatively acidic C–H bonds. Upon coordination to the palladium center, the C–H bond was deprotonated by carbonates or phosphates. In this regard, the relatively weak donation of Pfaltz ligand and Difluorophos was important to the successful activation of azoles. It should be cautioned that in examples of both Schemes 17 and 18, an alternative pathway is possible—azolyl palladation on a second palladium(II) center and subsequentazolyl transfer to the alkyl palladium(II) species for C–C coupling.

The *n*CMD pathway also operated in rhodium(I)-catalyzed conjugate addition of azoles (Scheme 19), including oxazoles, thiazoles, imidazoles and their benzofused derivatives.^{79,80} A rhodium(I) carboxylate complex of Xyl–P–Phos promoted C–H activation of pyridine *N*-oxides, (benzo)oxazoles and (benzo)thiazoles; the resulting heteroaryl rhodium(I) species then readily inserted into Michael acceptors (acrylate and acrylonitrile). The C7-substituents were necessary to weaken the coordination of azoles, so that C2 metalation can proceed. Deuterium labelling experiments (see Scheme 19B and C) revealed that after heteroaryl insertion of methacrylate, rapid β -hydride elimination and reinsertion, which is quite common in examples of rhodium catalysis, occurred to give β -rhodaacrylate species. Subsequent β -protonation resulted in partial deuteration at both β C–H bonds. This result is inconsistent with a simple pathway consisting of heteroaryl insertion and α -protonation of the resulting enolates.

4. σ -Bond metathesis of azaarenes by d^0 early metal complexes

σ -Bond metathesis occurs between a metal–ligand σ -bond and another single bond, *e.g.*, H–H, B–H, Si–H and C–H bonds. This kind of reactivity is mainly limited to transition metal complexes of metals with d^0 configuration, which cannot transfer electron density to single bonds of these substrates. For example, lanthanide alkyl complexes were known to undergo facile σ -bond metathesis with dihydrogen and polar XH single bonds (X = O, N, S).

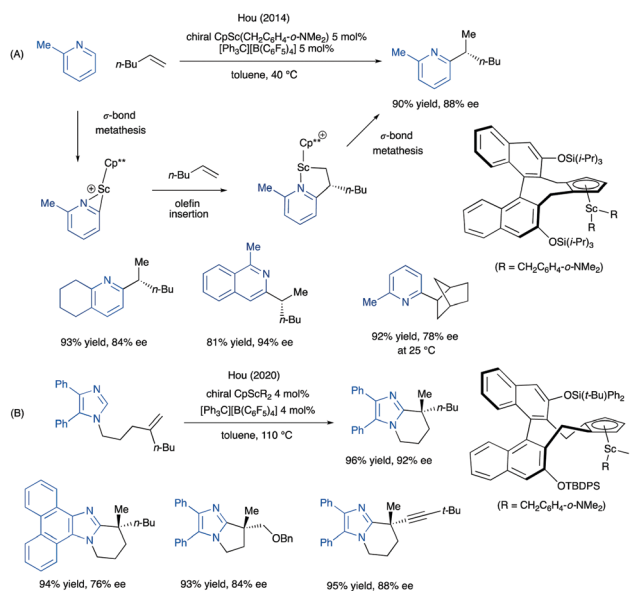


Scheme 19 Asymmetric conjugate heteroarylation of α -substituted acrylates enabled by Rh(I).

Half-sandwich alkyl complexes of rare earth metals (scandium, ytterbium and lanthanides) were shown to undergo σ -bond metathesis with *ortho*-C–H bonds of pyridines and other azaarenes. The resulting azaaryl metal species have been successfully added to several types of alkenes including ethylene, norbornene, α -olefins, styrenes, allenes and 1,3-dienes.^{81,82} Recently, a chiral cyclopentadienyl complex of dialkylscandium(III) was developed to promote asymmetric *o*'-alkylation of *o*-substituted pyridines with α -olefins (Scheme 20A).⁸³ Without *ortho*-groups on pyridine, double 2,6-alkylation took place. Under other conditions, σ -bond metathesis may give way to iterative insertion of alkenes resulting in olefin polymerization. Later, the same chiral cyclopentadienyl scandium catalyst was applied to olefinic cyclization of imidazoles (Scheme 20B).⁸⁴

5. Wacker-type activation of olefins by electrophilic late metal complexes

Both Pt(II) and Au(I) complexes were highly carbophilic towards electron-neutral alkenes and alkynes, owing to relativistic effect.^{85–88} The activated electron-neutral alkynes and alkenes can thus undergo Wacker-type attack by weak nucleophiles such as alcohols, arylamines, indoles and pyrroles. These reactions bypassed the intermediacy of heteroaryl metal species. Most of reported examples so far capitalized on high efficiency of intramolecular cyclization of indoles and pyrroles on alkenes to form 5- or 6-membered rings. Analogous intermolecular attack, however, is more challenging. In most of examples described below, *gem*-dimethyl groups or malonate groups were



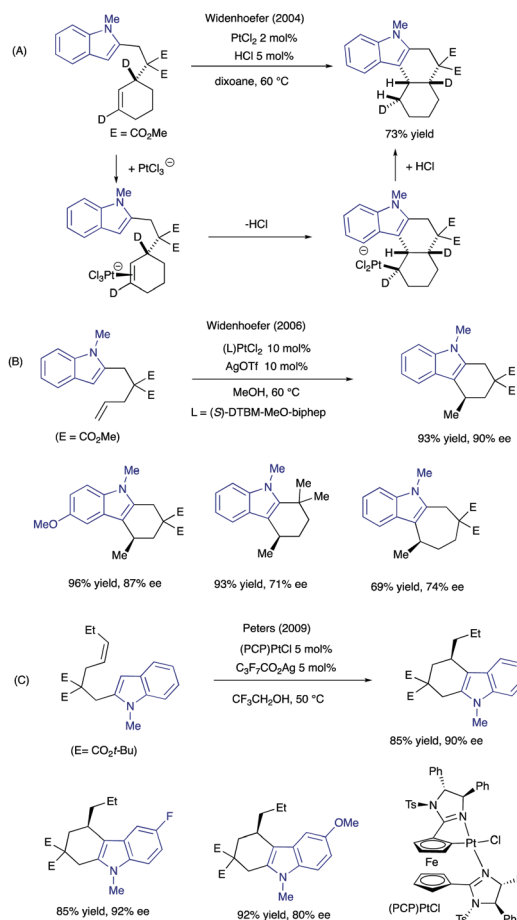
Scheme 20 Enantioselective C–H alkylation of *o*-substituted pyridines and imidazoles with alkenes catalyzed by a chiral half-sandwich complex of scandium.

purposefully installed on linkers to enhance the cyclization efficiency benefiting from Thorpe–Ingold effect.

In 2004, platinum dichloride was reported to promote intramolecular C3-alkylation of indoles with pendent alkenes and a deuterium labelling experiment indicated that the reaction proceeded *via* outer-sphere nucleophilic attack (Scheme 21A).⁸⁹ Later, an asymmetric variant of this process was promoted by a platinum complex of DTBM–MeO–BIPHEP (Scheme 21B).⁹⁰ In the third example, a cationic NCN-type platinum complex was the active catalyst to activate alkenes (Scheme 21C).⁹¹ Notably, the use of 2,2,2-trifluoroethanol solvent significantly improved the efficiency of the reactions by stabilizing cationic metal species as the active catalysts, but in methanol the product was produced in only 14% yield.

In gold(I)-catalyzed intramolecular indole substitution of allylic alcohols, the active catalyst, a dicationic diaura complex of DTBM–MeO–biphep, was generated *in situ* via halide abstraction by silver triflate (Scheme 22).^{92,93} The (*Z*)-geometry of alkenols were important to good reactivity and good stereoselectivity. In comparison, the corresponding (*E*)-isomer only led to a trace amount of the product. In subsequent mechanistic studies, the indolyl N–hydrogen also proved essential for the catalytic process; without it, no cyclization occurred. In combination with DFT calculations, a revised reaction pathway was proposed. After indole addition to the bound olefin, indolyl C2–hydrogen shifted to the hydroxyl group. The departure of the resulting water was also assisted by a hydrogen-bonding network consisting triflate ion and the indolyl N–H bond. The second gold center is believed to act as a structural element, without participating directly in the step of C–O bond breakage.

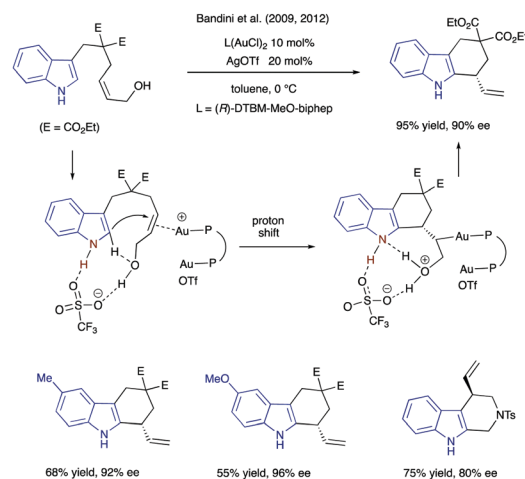
In recent years, significant advancement was made in enantioselective intermolecular Wacker-type reactions by using palladium catalysts. In Pd(II)-catalyzed C–H activation reactions,



Scheme 21 Pt(II)-catalyzed annulation of indoles with tethered alkenes.

N-8-quinolyl amides were often utilized to readily form palladacycles, which can enable selective activation of aliphatic C–H bonds on the amides.^{94,95} With this knowledge, an alkene group on the amide chains may be stereoselectively approached by external nucleophiles such as indoles. The challenge to realize such a stereoselective process is to find a chiral monodentate ligand, since only the fourth coordination site is left available in the palladacycle.

Extensive catalyst design and screening eventually culminated in the discovery of chiral monooxazolines MOXin and MOXca, which have large indolylmethyl and carbazolylmethyl side chains, respectively. A daunting task in coordination chemistry was thus accomplished! In the examples of hydroindoylation, indole attacked at the distal carbon of the (*E*)-alkene to give a stable five-membered palladacycle, which helped to impede β -hydrogen elimination, an obvious side reaction (Scheme 23A).⁹⁶ In subsequent studies of carboborylation, surprisingly both (*Z*)- and (*E*)-isomers afforded the same *syn*-diastereomers exclusively with identical ee values, despite that the reaction of the (*E*)-isomers was conducted in slightly modified conditions (KF in 1:1 HFIP/THF at 60 °C) (Scheme 23B and C).^{97–100} The result revealed that a fast equilibrium between the two olefinic isomers existed under catalytic conditions, in which the *cis*-isomers were the actual substrates for nucleophilic attack.



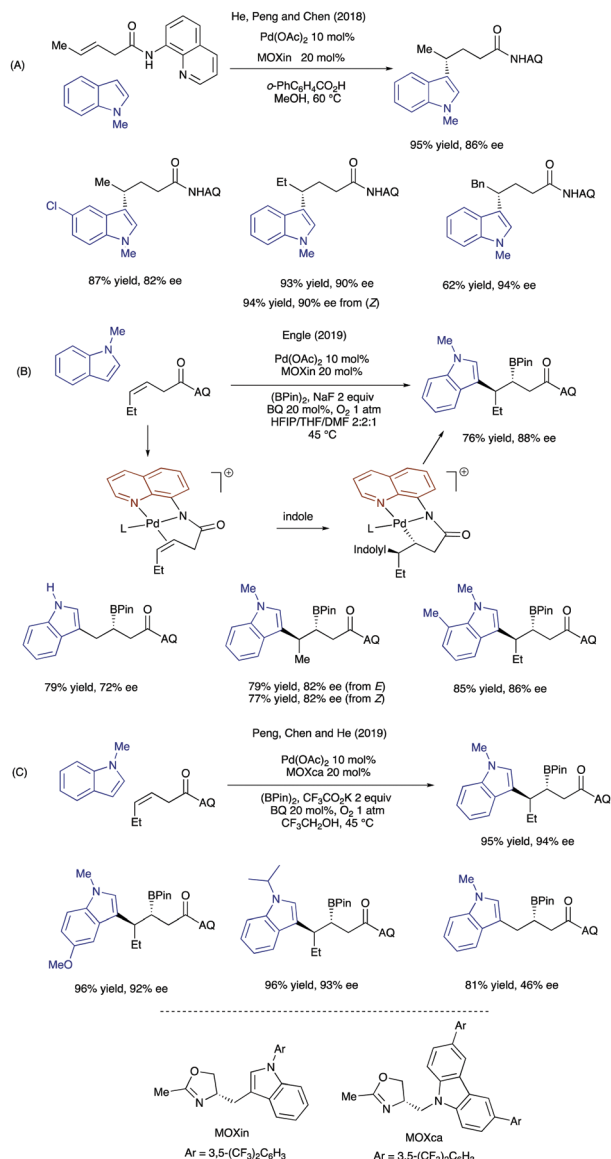
Scheme 22 Au(I)-catalyzed asymmetric cyclization of indoles with allylic alcohols.

In another front of research, palladium(II) catalysts ligated by weakly donating variants of MeO-biphep were recently discovered to promote Wacker-type three-component couplings of propargylic acetates and cycloalkenes (Scheme 24).^{101,102} Unlike the aforementioned examples, no directing group was necessary on olefins to restrict the conformation of olefins for stereoselective attack of nucleophiles. After oxidative addition, the resulting π -allenyl complex can exist in equilibrium with the σ -type form upon cycloolefin binding, but no Heck insertion ensued. Instead, external weak nucleophiles such as alcohols and arylamines attacked at the bound olefins to trigger three-component couplings with the allenyl fragment. Later, the Wacker reactivity was extended to nucleophilic arenes and heteroarenes including indoles, pyrroles and some activated thiophenes, furans and anilines. The 2-furyl and benzofuryl groups on the phosphorus atoms of MeO-biphep ligands are electron-withdrawing in nature which proved crucial to ensuring Wacker-type reactivity. In comparison, a palladium catalyst of the parent MeO-biphep showed very low catalytic activity.

6. Metal hydride reaction manifolds

Metal hydride complexes can readily add to unsaturated bonds such as styrene and conjugated dienes and initiate C–C couplings with heteroarenes. The resulting benzyl complexes of copper, for examples, are nucleophilic and can add to a heteroarene possessing a leaving group or add to an electrophilic azine. On the other hand, η^3 -allyl complexes of rhodium and nickel, *in situ* formed, can serve as acceptors for attack by external nucleophiles such as indole.

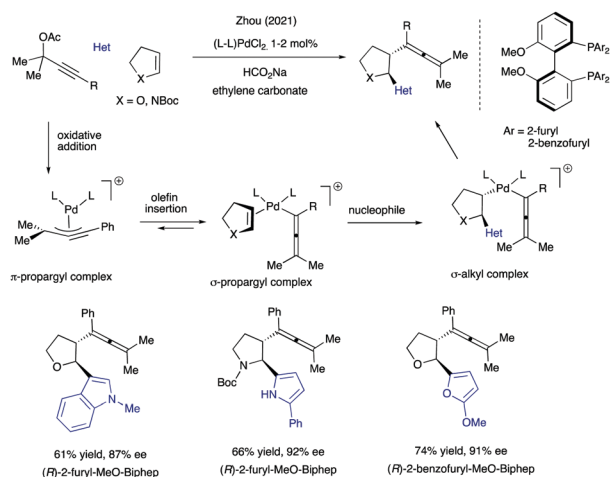
Copper hydride complexes ligated by chiral bulky diphosphines (*e.g.*, Tangphos and DTBM-Segphos) can add to styrene to produce enantio-enriched *sec*-benzyl complexes which then intercepted various electrophiles in catalytic manifolds.^{103–105} For example, Ge *et al.* reported that chiral benzyl copper species added to reactive heteroarenes such as quinoline *N*-oxides (Scheme 25A).¹⁰⁶ Similarly, Buchwald *et al.* reported that a



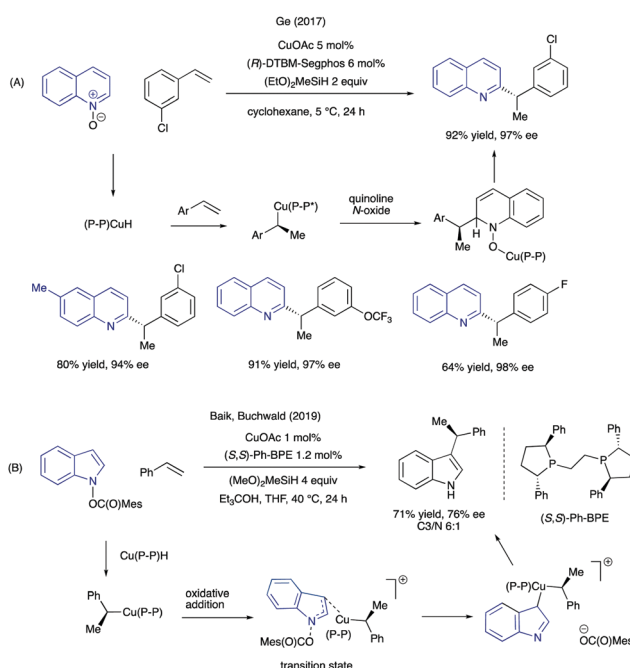
Scheme 23 Pd(II)-catalyzed enantioselective Wacker-type attack of indoles on alkenyl amides.

copper/Ph-BPE catalyst promoted C3-selective benzylation of *N*-(benzoyloxy)indoles (Scheme 25B).¹⁰⁷ DFT calculation suggested that steric bulkiness of Ph-BPE dictated that oxidation addition occurred favorably at the indolyl C3 position rather than on its nitrogen. In analogous reactions promoted by a copper complex of DTBM-Segphos, the regioselectivity switched to *N*-benzylation. DFT calculations suggested that in this case steric interaction was less important and thus the oxidative addition occurred selectively at the nitrogen due to its high intrinsic electrophilicity. Recently, the manifold of chiral benzyl copper species was successfully extended to pyridines and pyridazines¹⁰⁸ and stereoselective allylation of *N*-pivaloyl benzimidazoles was also realized *via* copper hydride addition to 1,3-dienes.¹⁰⁹

The η³-allyl complex of rhodium produced from hydride insertion was electrophilic and can be attacked by nucleophilic indoles (Scheme 26).¹¹⁰ A rhodium complex of a chiral PCP-



Scheme 24 Pd-catalyzed three-component coupling of heteroarenes, cycloalkenes and propargylic acetates.

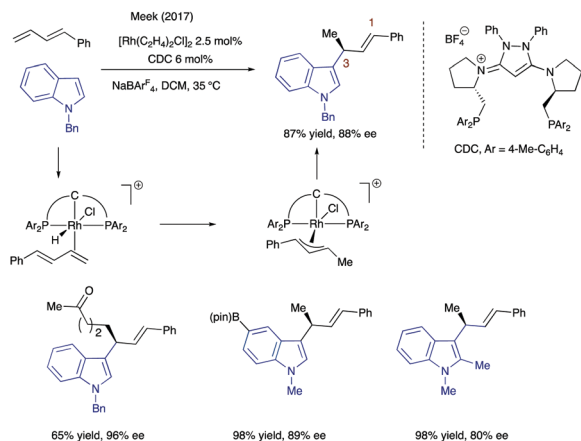


Scheme 25 Enantioselective allylation of quinoline *N*-oxides and indole derivatives using styrenes catalyzed by copper.

pincer carbodicarbene was deployed to form a deep chiral pocket. Hydride insertion occurred selectively to give an enantiotopic π-allyl complex. Subsequent indole attack with a preference for the alkyl-substituted terminus with >10:1 regioselectivity. Very recently, Zhou *et al.* also reported that nickel hydride catalysts promoted similar regio- and stereoselective addition of indoles to aliphatic 1,3-dienes.¹¹¹

7. Conclusion

In summary, this review captures the main development in the field of asymmetric hydroheteroarylation of alkenes that were



Scheme 26 Asymmetric hydroheteroarylation of 1,3-dienes with indoles catalyzed by rhodium.

assisted by transition metal complexes over the last two decades (see Fig. 2). Previously well-established reaction mechanisms were successfully adopted to enantioselective transformations, examples including electrophilic palladation of indole, σ -bond metathesis with pyridine and Wacker-type activation of alkenes. In these endeavors, new classes of chiral ligands were invented or adopted to tackle the challenge of the stereoinduction during bond formation. Examples include bulky monodentate oxazolines for Wacker-type reactions, chiral Pyrox ligands for palladium-catalyzed stereoselective β -insertion and chiral variants of cyclopentadienyl to construct half-sandwich complexes of scandium.

More importantly, several *new* mechanisms for C–H bond activation were exploited to activate (hetero)arenes in asymmetric alkylation reactions. Such examples include concerted oxidative addition of (hetero)aryl C–H bonds by low-valent rhodium(i) and iridium(i) complexes, ligand-to-ligand hydrogen transfer on 3d metals such as nickel, which bypasses formal oxidative addition, concerted or nonconcerted metalation deprotonation of (hetero)aryl C–H bonds by palladium(ii). In the examples of nickel(0)-catalyzed heteroarylation of olefins, the benefit of using extremely large NHC ligands to enforce the LLHT were duly recognized. Subsequent invention of extremely large, C_2 -symmetric NHCs has enabled stereoselective *endo*-cyclizations on pyridines and indoles. In another example, a secondary phosphine oxide present in a special Josiphos can have agostic interaction with nickel(0) center and thus, support a novel reaction pathway involving P–H oxidative addition and subsequent LLHT.

The aforementioned examples clearly illustrate how in-depth understanding of metal reactivity and innovation in new ancillary ligands worked hand-in-hand to achieve asymmetric heteroarylation of alkenes, those challenging, yet useful processes. In future, we anticipate some new developments following footsteps of recent breakthroughs as follows. (a) Recently, nickel(0) complexes of chiral NHCs successfully catalyzed asymmetric 6-*endo*-cyclization of azacycles *via* LLHT pathways. Can the nickel catalysts be applied to intermolecular heteroarylation of alkenes, for example, 1,1-disubstituted

alkenes that add alkyl chains possessing β -stereocenters? (b) Asymmetric Pd-catalyzed domino couplings *via* nCMD have been achieved with oxadiazoles, a special type of azaheterocycles. It remains to be seen if other types of azoles containing acidified C–H bonds can be used, such as (benzo)thiazole, (benzo)oxazole and even thiophene. (c) Palladium(ii) catalysts ligated by weakly coordinating MeO–BIPHEP have been reported to catalyze three-component Wacker-type attack on simple cycloalkenes. It will be desirable if the reactivity can be extended to acyclic alkenes and 1,3-dienes. (d) Very recently, palladacycles, *in situ* generated from *N*-8-quinolylamides, enabled asymmetric Wacker-type attack (*e.g.*, by indoles) on pendent alkenes, which eventually resulted in hydroheteroarylation and carboborylation. We expect to see similar Wacker manifolds in the near future that are terminated by C–C cross-couplings, for example, alkynylation, azoloylation and cyanation.

Author contributions

Both ST and JSZ contributed to the conceptualization and writing of this review.

Conflicts of interest

There are no conflicts to declare.

Acknowledgements

We acknowledge financial supports from Peking University Shenzhen Graduate School, State Key Laboratory of Chemical Oncogenomics, Guangdong Provincial Key Laboratory of Chemical Genomics, Shanghai Key Laboratory for Molecular Engineering of Chiral Drugs and Shenzhen Bay Laboratory for JSZ and Nanyang Technological University for ST.

Notes and references

- 1 T. K. Warren, J. Wells, R. G. Panchal, K. S. Stuthman, N. L. Garza, S. A. Van Tongeren, L. Dong, C. J. Retterer, B. P. Eaton, G. Pegoraro, S. Honnold, S. Bantia, P. Kotian, X. Chen, B. R. Taubenheim, L. S. Welch, D. M. Minning, Y. S. Babu, W. P. Sheridan and S. Bavari, *Nature*, 2014, **508**, 402–405.
- 2 C. Scavone, S. Brusco, M. Bertini, L. Sportiello, C. Rafaniello, A. Zoccoli, L. Berrino, G. Racagni, F. Rossi and A. Capuano, *Br. J. Pharmacol.*, 2020, **177**, 4813–4824.
- 3 R. G. Bakker-Arkema, M. H. Davidson, R. J. Goldstein, J. Davignon, J. L. Isaacsohn, S. R. Weiss, L. M. Keilson, W. V. Brown, V. T. Miller, L. J. Shurzinske and D. M. Black, *JAMA*, 1996, **275**, 128–133.
- 4 R. W. Fitch, T. F. Spande, H. M. Garraffo, H. J. C. Yeh and J. W. Daly, *J. Nat. Prod.*, 2010, **73**, 331–337.
- 5 M. M. Heravi, V. Zadsirjan, B. Masoumi and M. Heydari, *J. Organomet. Chem.*, 2019, **879**, 78–138.

- 6 T. B. Poulsen and K. A. Jørgensen, *Chem. Rev.*, 2008, **108**, 2903–2915.
- 7 G. Evano and C. Theunissen, *Angew. Chem., Int. Ed.*, 2019, **58**, 7202–7236.
- 8 P. Gandeepan, T. Müller, D. Zell, G. Cera, S. Warratz and L. Ackermann, *Chem. Rev.*, 2019, **119**, 2192–2452.
- 9 J. Loup, U. Dhawa, F. Pesciaioli, J. Wencel-Delord and L. Ackermann, *Angew. Chem., Int. Ed.*, 2019, **58**, 12803–12818.
- 10 Z. Dong, Z. Ren, S. J. Thompson, Y. Xu and G. Dong, *Chem. Rev.*, 2017, **117**, 9333–9403.
- 11 T. K. Achar, S. Maiti, S. Jana and D. Maiti, *ACS Catal.*, 2020, **10**, 13748–13793.
- 12 G. Evano and C. Theunissen, *Angew. Chem., Int. Ed.*, 2019, **58**, 7558–7598.
- 13 M. Gómez-Gallego and M. A. Sierra, *Chem. Rev.*, 2011, **111**, 4857–4963.
- 14 D. Balcells, E. Clot and O. Eisenstein, *Chem. Rev.*, 2010, **110**, 749–823.
- 15 X. Zhang, L. W. Chung and Y.-D. Wu, *Acc. Chem. Res.*, 2016, **49**, 1302–1310.
- 16 C. Shan, R. Bai and Y. Lan, *Acta Phys.-Chim. Sin.*, 2019, **35**, 940–953.
- 17 Y.-F. Yang, X. Hong, J.-Q. Yu and K. N. Houk, *Acc. Chem. Res.*, 2017, **50**, 2853–2860.
- 18 K. D. Vogiatzis, M. V. Polynski, J. K. Kirkland, J. Townsend, A. Hashemi, C. Liu and E. A. Pidko, *Chem. Rev.*, 2019, **119**, 2453–2523.
- 19 D. Gallego and A. Baquero Edwin, *Open Chem.*, 2018, **16**, 1001–1058.
- 20 F. Naoaki, K. Fumitoshi, Y. Airi, C. Naoto and M. Shinji, *Chem. Lett.*, 1997, 425–426.
- 21 D. A. Colby, A. S. Tsai, R. G. Bergman and J. A. Ellman, *Acc. Chem. Res.*, 2012, **45**, 814–825.
- 22 B. A. Arndtsen, R. G. Bergman, T. A. Mobley and T. H. Peterson, *Acc. Chem. Res.*, 1995, **28**, 154–162.
- 23 R. K. Thalji, J. A. Ellman and R. G. Bergman, *J. Am. Chem. Soc.*, 2004, **126**, 7192–7193.
- 24 R. M. Wilson, R. K. Thalji, R. G. Bergman and J. A. Ellman, *Org. Lett.*, 2006, **8**, 1745–1747.
- 25 A. S. Tsai, R. M. Wilson, H. Harada, R. G. Bergman and J. A. Ellman, *Chem. Commun.*, 2009, 3910–3912.
- 26 Ł. Woźniak, J.-F. Tan, Q.-H. Nguyen, A. Madron du Vigné, V. Smal, Y.-X. Cao and N. Cramer, *Chem. Rev.*, 2020, **120**, 10516–10543.
- 27 C. S. Sevov and J. F. Hartwig, *J. Am. Chem. Soc.*, 2013, **135**, 2116–2119.
- 28 C. S. Sevov, J. Zhou and J. F. Hartwig, *J. Am. Chem. Soc.*, 2012, **134**, 11960–11963.
- 29 M. Hatano, Y. Ebe, T. Nishimura and H. Yorimitsu, *J. Am. Chem. Soc.*, 2016, **138**, 4010–4013.
- 30 S. Grélaud, P. Cooper, L. J. Feron and J. F. Bower, *J. Am. Chem. Soc.*, 2018, **140**, 9351–9356.
- 31 D. Xing and G. Dong, *J. Am. Chem. Soc.*, 2017, **139**, 13664–13667.
- 32 Z. Wang, B. J. Reinius and G. Dong, *J. Am. Chem. Soc.*, 2012, **134**, 13954–13957.
- 33 F. Mo and G. Dong, *Science*, 2014, **345**, 68–72.
- 34 X.-Y. Bai, Z.-X. Wang and B.-J. Li, *Angew. Chem., Int. Ed.*, 2016, **55**, 9007–9011.
- 35 X.-Y. Bai, W.-W. Zhang, Q. Li and B.-J. Li, *J. Am. Chem. Soc.*, 2018, **140**, 506–514.
- 36 Z. Yu, L. Meng and Z. Lin, *Organometallics*, 2019, **38**, 2998–3006.
- 37 X. Li, H. Wu, Y. Lang and G. Huang, *Catal. Sci. Technol.*, 2018, **8**, 2417–2426.
- 38 G. Huang and P. Liu, *ACS Catal.*, 2016, **6**, 809–820.
- 39 J. Guihaumé, S. Halbert, O. Eisenstein and R. N. Perutz, *Organometallics*, 2012, **31**, 1300–1314.
- 40 J. S. Bair, Y. Schramm, A. G. Sergeev, E. Clot, O. Eisenstein and J. F. Hartwig, *J. Am. Chem. Soc.*, 2014, **136**, 13098–13101.
- 41 Y. Schramm, M. Takeuchi, K. Semba, Y. Nakao and J. F. Hartwig, *J. Am. Chem. Soc.*, 2015, **137**, 12215–12218.
- 42 S. Tang, O. Eisenstein, Y. Nakao and S. Sakaki, *Organometallics*, 2017, **36**, 2761–2771.
- 43 N. I. Saper, A. Ohgi, D. W. Small, K. Semba, Y. Nakao and J. F. Hartwig, *Nat. Chem.*, 2020, **12**, 276–283.
- 44 J. Diesel, D. Grosheva, S. Kodama and N. Cramer, *Angew. Chem., Int. Ed.*, 2019, **58**, 11044–11048.
- 45 W.-B. Zhang, X.-T. Yang, J.-B. Ma, Z.-M. Su and S.-L. Shi, *J. Am. Chem. Soc.*, 2019, **141**, 5628–5634.
- 46 Y. Cai, X. Ye, S. Liu and S.-L. Shi, *Angew. Chem., Int. Ed.*, 2019, **58**, 13433–13437.
- 47 S. Okumura, S. Tang, T. Saito, K. Semba, S. Sakaki and Y. Nakao, *J. Am. Chem. Soc.*, 2016, **138**, 14699–14704.
- 48 J. Loup, V. Müller, D. Ghorai and L. Ackermann, *Angew. Chem., Int. Ed.*, 2019, **58**, 1749–1753.
- 49 J.-B. Liu, X. Wang, A. M. Messinis, X.-J. Liu, R. Kuniyil, D.-Z. Chen and L. Ackermann, *Chem. Sci.*, 2021, **12**, 718–729.
- 50 R. N. Perutz and S. Sabo-Etienne, *Angew. Chem., Int. Ed.*, 2007, **46**, 2578–2592.
- 51 Y.-X. Wang, S.-L. Qi, Y.-X. Luan, X.-W. Han, S. Wang, H. Chen and M. Ye, *J. Am. Chem. Soc.*, 2018, **140**, 5360–5364.
- 52 B. J. Fallon, E. Derat, M. Amatore, C. Aubert, F. Chemla, F. Ferreira, A. Perez-Luna and M. Petit, *J. Am. Chem. Soc.*, 2015, **137**, 2448–2451.
- 53 C.-S. Wang, S. Di Monaco, A. N. Thai, M. S. Rahman, B. P. Pang, C. Wang and N. Yoshikai, *J. Am. Chem. Soc.*, 2020, **142**, 12878–12889.
- 54 P.-S. Lee and N. Yoshikai, *Org. Lett.*, 2015, **17**, 22–25.
- 55 J. Loup, D. Zell, J. C. A. Oliveira, H. Keil, D. Stalke and L. Ackermann, *Angew. Chem., Int. Ed.*, 2017, **56**, 14197–14201.
- 56 T. Rogge, J. C. A. Oliveira, R. Kuniyil, L. Hu and L. Ackermann, *ACS Catal.*, 2020, **10**, 10551–10558.
- 57 D. Zell, M. Bursch, V. Müller, S. Grimme and L. Ackermann, *Angew. Chem., Int. Ed.*, 2017, **56**, 10378–10382.
- 58 E. Tan, O. Quinonero, M. Elena de Orbe and A. M. Echavarren, *ACS Catal.*, 2018, **8**, 2166–2172.
- 59 B. P. Carrow, J. Sampson and L. Wang, *Isr. J. Chem.*, 2020, **60**, 230–258.

- 60 L. Wang and B. P. Carrow, *ACS Catal.*, 2019, **9**, 6821–6836.
- 61 D. Lapointe and K. Fagnou, *Chem. Lett.*, 2010, **39**, 1118–1126.
- 62 S. I. Gorelsky, D. Lapointe and K. Fagnou, *J. Am. Chem. Soc.*, 2008, **130**, 10848–10849.
- 63 D. L. Davies, S. M. A. Donald and S. A. Macgregor, *J. Am. Chem. Soc.*, 2005, **127**, 13754–13755.
- 64 Y. Boutadla, D. L. Davies, S. A. Macgregor and A. I. Poblador-Bahamonde, *Dalton Trans.*, 2009, 5820–5831.
- 65 D. L. Davies, S. A. Macgregor and C. L. McMullin, *Chem. Rev.*, 2017, **117**, 8649–8709.
- 66 A. Petit, J. Flygare, A. T. Miller, G. Winkel and D. H. Ess, *Org. Lett.*, 2012, **14**, 3680–3683.
- 67 V. Gandon and C. Hoarau, *J. Org. Chem.*, 2021, **86**, 1769–1778.
- 68 J. M. Joo, B. B. Touré and D. Sames, *J. Org. Chem.*, 2010, **75**, 4911–4920.
- 69 E. M. Ferreira and B. M. Stoltz, *J. Am. Chem. Soc.*, 2003, **125**, 9578–9579.
- 70 M. A. Abozeid, S. Sairenji, S. Takizawa, M. Fujita and H. Sasai, *Chem. Commun.*, 2017, **53**, 6887–6890.
- 71 C. Zhang, C. B. Santiago, J. M. Crawford and M. S. Sigman, *J. Am. Chem. Soc.*, 2015, **137**, 15668–15671.
- 72 T.-S. Mei, H. H. Patel and M. S. Sigman, *Nature*, 2014, **508**, 340–344.
- 73 O. René, D. Lapointe and K. Fagnou, *Org. Lett.*, 2009, **11**, 4560–4563.
- 74 U. K. Sharma, N. Sharma, Y. Kumar, B. K. Singh and E. V. Van der Eycken, *Chem. – Eur. J.*, 2016, **22**, 481–485.
- 75 Y. Ping, Y. Li, J. Zhu and W. Kong, *Angew. Chem., Int. Ed.*, 2019, **58**, 1562–1573.
- 76 W. Kong, Q. Wang and J. Zhu, *J. Am. Chem. Soc.*, 2015, **137**, 16028–16031.
- 77 S. Tong, A. Limouni, Q. Wang, M.-X. Wang and J. Zhu, *Angew. Chem., Int. Ed.*, 2017, **56**, 14192–14196.
- 78 X. Bao, Q. Wang and J. Zhu, *Angew. Chem., Int. Ed.*, 2017, **56**, 9577–9581.
- 79 C. M. Filloux and T. Rovis, *J. Am. Chem. Soc.*, 2015, **137**, 508–517.
- 80 J. Ryu, S. H. Cho and S. Chang, *Angew. Chem., Int. Ed.*, 2012, **51**, 3677–3681.
- 81 G. Luo, Y. Luo, J. Qu and Z. Hou, *Organometallics*, 2012, **31**, 3930–3937.
- 82 M. Nishiura, F. Guo and Z. Hou, *Acc. Chem. Res.*, 2015, **48**, 2209–2220.
- 83 G. Song, W. N. O. Wylie and Z. Hou, *J. Am. Chem. Soc.*, 2014, **136**, 12209–12212.
- 84 S.-J. Lou, Z. Mo, M. Nishiura and Z. Hou, *J. Am. Chem. Soc.*, 2020, **142**, 1200–1205.
- 85 A. R. Chianese, S. J. Lee and M. R. Gagné, *Angew. Chem., Int. Ed.*, 2007, **46**, 4042–4059.
- 86 A. Fürstner and P. W. Davies, *Angew. Chem., Int. Ed.*, 2007, **46**, 3410–3449.
- 87 A. S. K. Hashmi and G. J. Hutchings, *Angew. Chem., Int. Ed.*, 2006, **45**, 7896–7936.
- 88 A. M. Echavarren, M. E. Muratore, V. López-Carrillo, A. Escribano-Cuesta, N. Huguet and C. Obradors, *Org. React.*, 2017, 1–288.
- 89 C. Liu, X. Han, X. Wang and R. A. Widenhoefer, *J. Am. Chem. Soc.*, 2004, **126**, 3700–3701.
- 90 X. Han and R. A. Widenhoefer, *Org. Lett.*, 2006, **8**, 3801–3804.
- 91 H. Huang and R. Peters, *Angew. Chem., Int. Ed.*, 2009, **48**, 604–606.
- 92 M. Bandini and A. Eichholzer, *Angew. Chem., Int. Ed.*, 2009, **48**, 9533–9537.
- 93 M. Bandini, A. Bottoni, M. Chiarucci, G. Cera and G. P. Miscione, *J. Am. Chem. Soc.*, 2012, **134**, 20690–20700.
- 94 S.-Y. Zhang, Q. Li, G. He, W. A. Nack and G. Chen, *J. Am. Chem. Soc.*, 2013, **135**, 12135–12141.
- 95 X. Zhang, G. Lu, M. Sun, M. Mahankali, Y. Ma, M. Zhang, W. Hua, Y. Hu, Q. Wang, J. Chen, G. He, X. Qi, W. Shen, P. Liu and G. Chen, *Nat. Chem.*, 2018, **10**, 540–548.
- 96 H. Wang, Z. Bai, T. Jiao, Z. Deng, H. Tong, G. He, Q. Peng and G. Chen, *J. Am. Chem. Soc.*, 2018, **140**, 3542–3546.
- 97 Z. Bai, S. Zheng, Z. Bai, F. Song, H. Wang, Q. Peng, G. Chen and G. He, *ACS Catal.*, 2019, **9**, 6502–6509.
- 98 Z. Liu, T. Zeng, K. S. Yang and K. M. Engle, *J. Am. Chem. Soc.*, 2016, **138**, 15122–15125.
- 99 Z. Liu, X. Li, T. Zeng and K. M. Engle, *ACS Catal.*, 2019, **9**, 3260–3265.
- 100 Z. Liu, H.-Q. Ni, T. Zeng and K. M. Engle, *J. Am. Chem. Soc.*, 2018, **140**, 3223–3227.
- 101 S. Teng, Y. R. Chi and J. S. Zhou, *Angew. Chem., Int. Ed.*, 2021, **60**, 4491–4495.
- 102 S. Teng, Z. Jiao, Y. R. Chi and J. S. Zhou, *Angew. Chem., Int. Ed.*, 2020, **59**, 2246–2250.
- 103 R. Y. Liu and S. L. Buchwald, *Acc. Chem. Res.*, 2020, **53**, 1229–1243.
- 104 D. Noh, H. Chea, J. Ju and J. Yun, *Angew. Chem., Int. Ed.*, 2009, **48**, 6062–6064.
- 105 S. Zhu, N. Niljianskul and S. L. Buchwald, *J. Am. Chem. Soc.*, 2013, **135**, 15746–15749.
- 106 S. Yu, H. L. Sang and S. Ge, *Angew. Chem., Int. Ed.*, 2017, **56**, 15896–15900.
- 107 Y. Ye, S.-T. Kim, J. Jeong, M.-H. Baik and S. L. Buchwald, *J. Am. Chem. Soc.*, 2019, **141**, 3901–3909.
- 108 M. W. Gribble, S. Guo and S. L. Buchwald, *J. Am. Chem. Soc.*, 2018, **140**, 5057–5060.
- 109 J. L. Knippel, Y. Ye and S. L. Buchwald, *Org. Lett.*, 2021, **23**, 2153–2157.
- 110 J. S. Marcum, C. C. Roberts, R. S. Manan, T. N. Cervarich and S. J. Meek, *J. Am. Chem. Soc.*, 2017, **139**, 15580–15583.
- 111 L. Cheng, M.-M. Li, M.-L. Li, L.-J. Xiao, J.-H. Xie and Q.-L. Zhou, *CCS Chem.*, 2021, **3**, 3260–3267.